JOURNAL OF THERMOPHYSICS AND HEAT TRANSFER
Vol. 21, No. 3, July–September 2007

In-Plane Thermal Conductivity in Thin Carbon Fiber Composites

Carlos Silva,* Egidio (Ed) Marotta,† and Michael Schuller‡
Texas A&M University, College Station, Texas 77843
Larry Peel§
Texas A&M University—Kingsville, Kingsville, Texas 78363-8202
and
Mark O'Neill¶
ENTECH, Inc., Keller, Texas 76248

DOI: 10.2514/1.27859

The objective of this study was to determine whether fiber type, fiber angle, and filler material affected the in-plane thermal conductivity of thin (7–15 mils thickness) carbon fiber composites. Two sets of samples were tested: low thermal conductivity samples made with polyacrylonitrile-based fibers ($k = 6.8$ W/m · K) in Fiberglast epoxy resin, and high thermal conductivity samples fabricated with coal-pitch-based fibers ($k = 620$ W/m · K) in cyanate ester resin. Samples were fabricated from 0/90 woven cloths and warped to obtain a range of fiber-pattern angles from 25/ − 25 to 65/ − 65. The filler effect on thermal conductivity was evaluated on additional samples prepared with 10% volume fraction of graphite powder in the matrix. Thermal conductivity of the low thermal conductivity samples was in the range of 15–20 W/m · K and showed up to a 15% improvement when the angle of the fibers was varied. High thermal conductivity samples showed thermal conductivities between 60 and 150 W/m · K, with an improvement up to 60% when the angle of the fibers relative to the heat flux direction was changed from 0/90 to 25/ − 25. The samples with graphite powder did not show any enhancement in thermal performance. As potential alternatives, unidirectional tape and eGraf's Spreadershield® foils were also tested, showing good thermal performance.

Nomenclature

k	=	thermal conductivity, W/m · K
k/k_0	=	conductivity relative to that of the 0–90 sample
k_f, k_m	=	thermal conductivity of fiber and matrix, W/m · K
W	=	uncertainty, %
α	=	fiber angle relative to heat flux direction, deg
β	=	thermal conductivity ratio k_f/k_m
ν	=	fiber volume fraction, %

I. Introduction

CARBON fibers were first commercially produced in the late 1950s and since then have been employed in many applications. With an average of 6 times the tensile strength of high-strength alloy steel and two-thirds the weight of aluminum, carbon fiber composites (CFC) with an epoxy matrix have become the standard material for lightweight, high performance applications ranging from recreational sports to aerospace.

Polymer matrix CFCs are considered poor thermal conductors with k values on the order of 1 to 10 W/m · K. However, coal-pitch based carbon fibers have thermal conductivities up to 1000 W/m · K along the fiber direction, 2.5 times the thermal conductivity of copper. This type of fiber and its composites are therefore suitable for thermal management applications within microelectronic and aerospace industries.

One space-related application that makes use of coal-pitch based CFCs is satellite thermal radiators, including solar array radiators. Given that CFCs can be manufactured into thin sheets (0.127 mm or 5 mils thickness or less), while simultaneously remaining structurally sound with good thermal conductivity and high emissivity properties, they have emerged as an effective means for removing thermal energy from sources such as microelectronics and solar cells. They can radiate this thermal energy to space without adding prohibitive mass to the system. The heat transport capacity per areal unit mass of the CFC, though dependent on the radiator design, while superior to metals, is still low compared to more complex systems like microheat pipes.

The Texas Engineering Experiment Station (TEES), through its Center for Space Power (CSP), is supporting Entech in developing the Stretched Lens Array SquareRigger (SLASR) technology [1,2] maturation program in support of NASA's Vision for Space Exploration. CSP's primary goals are to develop alternative heat rejection technologies that will reduce the mass of the heat rejection elements of SLASR by 40%.

The basic thermal environment the SLASR must contend with is shown in Fig. 1. The main thermal input is solar insolation, though reflected and emitted radiation from the Earth or the moon is also significant. Although the infrared emissivity of the radiator material is important, it is not difficult to get high values of this parameter, meaning the most challenging task is to spread the heat laterally from the cell stack. Doing so effectively requires a high conductivity and low density material.

The radiator has two main functions: 1) conduct heat away from the cell stack, and 2) radiate that heat into space. In performing these functions, it is important that the radiator 1) has minimum mass,

Presented as Paper 3433 at the 9th AIAA/ASME Joint Thermophysics and Heat Transfer Conference, San Francisco, CA, 5–8 June 2006; received 16 September 2006; revision received 28 January 2007; accepted for publication 29 January 2007.

*Graduate Student, Department of Mechanical Engineering, 3123 TAMU. Student Member AIAA.
†Associate Research Professor, Department of Mechanical Engineering, 3123 TAMU. Associate Fellow AIAA.
‡Assistant Director, Center for Space Power, Texas Engineering Experiment Station, 3118 TAMU. Member AIAA.
§Associate Professor and Interim Chair, Department of Mechanical and Industrial Engineering, MSC 191. Member AIAA.
¶President, 1077 Chisolm Trail.

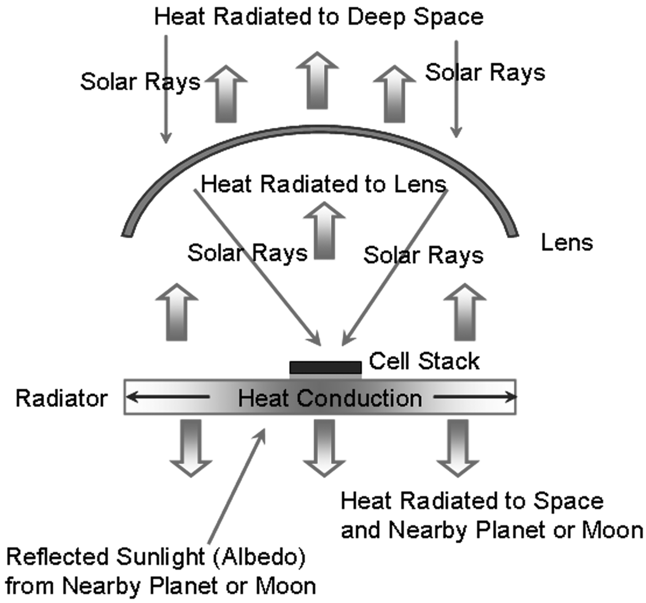

Fig. 1 The basic thermal environment for SLASR.

2) does not outgas detrimental substances, and 3) provides adequate stiffness to support the cell stack.

Entech's current approach to heat rejection uses Mitsubishi carbon fibers, woven into a cloth, and then formed into a composite using epoxy resin. The fibers in the cloth are woven at a 90 deg pitch, have a fiber conductivity of 620 $W/m \cdot K$, and an overall radiator thermal conductivity of 240 $W/m \cdot K$ as a composite. Figure 2 is a plot of radiator thickness versus aperture for fixed conditions and sets the baseline for comparison of alternative radiator materials.

CSP's goal in this research was to reduce the radiator mass by 40% without reducing performance (as measured by solar cell temperature). Two ways to achieve that goal are to 1) shift the line in Fig. 2 down and to the right, while maintaining cell temperature near 343 K (700°C), and 2) keep the line where it is, but reduce the density of the radiator material without reducing its thermal conductivity. We have focused on shifting the line in Fig. 2 for this project.

The current radiator has an areal density of 160 g/m^2 for the fibers and 210 g/m^2 for the composite. Our target areal density is 126 g/m^2 or lower for the overall radiator. CSP identified two main approaches to achieving this improvement: 1) improved materials and 2) hybrid radiator concepts.

The most straightforward way to improve radiator performance is by finding a higher conductivity or lower density material for the radiator. Figure 3 shows the trade-off between radiator areal mass density and conductivity. Assuming constant material density, the

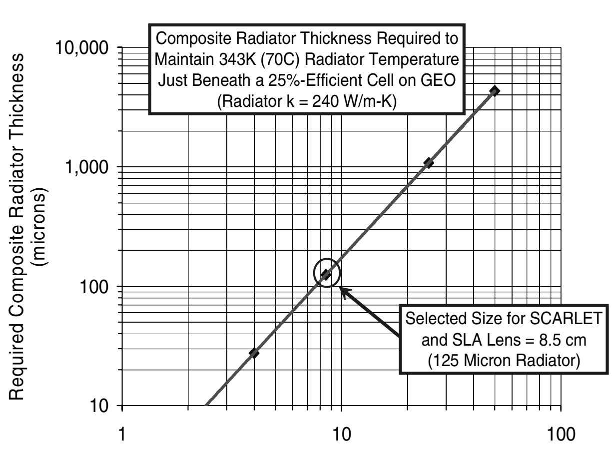

Fig. 2 Radiator thickness versus aperture width (current technology).

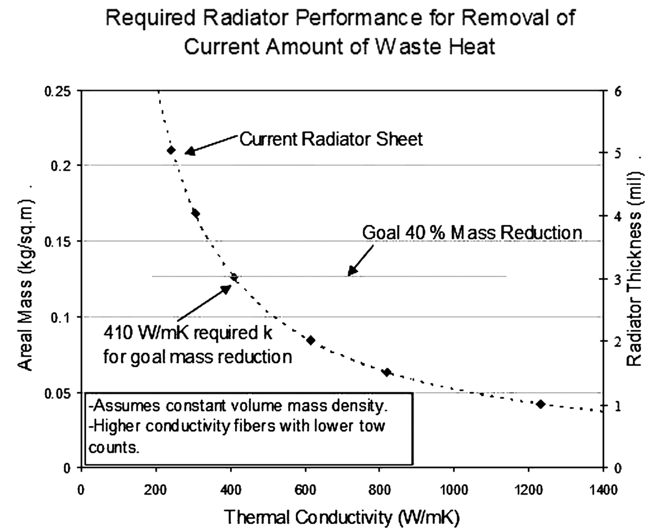

Fig. 3 Radiator areal mass/thickness versus thermal conductivity.

areal mass is proportional to thickness. We also assume that the heat load and temperature remain constant.

One other approach to improving the performance of the radiator without changing materials is to reorient the fibers in the cloth used to craft the composite (patterning). The experimental results presented in this report are based on this latter approach.

II. Literature Review

Past research studies have measured thermal conductivity values in CFCs as function of fiber type, volume fraction and size, and epoxy matrix material. Thermal conductivity has been measured in the transverse (across the fibers) and longitudinal (along the fibers) directions. However, none of the studies have focused on thin CFC sheets and the effect of weave angle on the effective thermal conductivity. The effect of fiber orientation was previously studied by Scott and Beck [3], but on low thermal conductivity AS4 (Hercules) fibers.

Mirmira et al. [4] studied the transverse and longitudinal thermal conductivity of graphite (carbon) fiber composites for a range of temperatures, pressures, and fiber volume fractions. They presented a comprehensive compilation of the theoretical models available, which was used as reference for developing an equation relating the thermal contact resistance of the CFC to the fiber and epoxy conductivities, fiber volume fraction, sample thickness, and microhardness.

Kulkarni and Brady [5] presented a model for global thermal conductivity based on the conductivity of the individual components of the CFC, fiber volume fraction, and orientation of the layers in the composite. This theoretical study considered composites with 10 to 45 layers, aligned in several different angles. No experimental data were reported.

Experimental investigations in thermal performance of CFC have been generally linked to specific applications within the microelectronic and aerospace industry. NASA [6] tested several CFC in single and multilayered 0/90 configurations, with both polyacrylonitrile (PAN) and coal-pitch fibers. Heat capacity, thermal diffusivity, and thermal conductivity were measured in the normal and in-plane directions over a temperature range from 20 to 1600°C.

Electrical and thermal conductivity of CFC were studied by Gaier et al. [7]. Both PAN (BP-Amoco) and coal-pitch (Thornel) fibers were used to fabricate 4-ply panels with alternating 0/90 and 0/0 angles. James et al. [8] investigated thermal conductivity of CFC made of GY70 (Cytec) fibers in epoxy resin. Ibrahim [9] studied the thermal performance of coal-pitch fiber reinforced composites for use as heat sinks in microelectronic packages. The thermal conductivity in the longitudinal direction was measured to be 412 $W/m \cdot K$ for the unidirectional plied CFC, while the transverse conductivity was 2 orders of magnitude lower (0.8 $W/m \cdot K$).

Jensen [10] performed an experimental study on CFC made with coal-pitch fibers (Thornel P-120) for thermal management in spacecrafts. Thermal conductivity averaged 300 and 1.0 $\mathrm{W/m \cdot K}$ in the longitudinal and transverse directions, respectively. All measurements were made in 300–400 K temperature range.

Peterson and Fletcher [11] presented a review in experimental and analytical work done on thermal conductivity of fiber composites. He studied the analytical and empirical relationships for in-plane thermal conductivity of Rayleigh [12], Maxwell [13], Soliman et al. [14], Singh et al. [15], and Alexander [16], as well as the rule of mixtures formulation, and compared them to the—limited—experimental data available at the time, finding reasonable agreement.

III. Objectives

In this experimental investigation, the thermal conductivity in CFC sheets ranging from 15 to 10 mils thickness was studied, and the influence of fiber type, fiber orientation, and filling material on the thermal performance was analyzed. Samples were made with Hexcel AS4 and Mitsubishi K13C fiber woven mats (published fiber conductivities are 6.8 and 620 $\mathrm{W/m \cdot K}$, respectively) in Fiberglast epoxy and cyanate ester epoxy matrices, and then tested for longitudinal conductivity. The effect of fiber orientation was explored for fiber angles ranging from $25/-25$ to $65/-65$ (in 5 deg increments) with respect to heat flow direction. Graphite powder filler was added to some samples to explore the effect of filling the cloth's pores and improving the conductivity of the matrix on overall conductivity and heat rejection. Additionally, thermal conductivity measurements were performed on a 7 mil thick unidirectional tape (all fibers oriented in the direction of heat flow).

We also identified a commercial product, eGraf spreadershield, which has the requisite thermal conductivity and can be made with a reflective coating to reduce solar/Earth shine absorption. It is not a stiff material, so additional measures would have to be taken to meet the structural requirements.

IV. Experimental Procedure

A. Sample Preparation

We fabricated several samples of composite using two different types of fiber and epoxy matrices as follows:

1) Low thermal conductivity (LTC) samples were fabricated with a Hexcel 282 woven mat made of PAN-based AS4 carbon fibers and cured with Fiberglast 2060 epoxy. Samples were made with angles of 0/90, $45/-45$, $60/-60$, and $30/-30$ deg with respect to the intended heat flow direction. Additional samples of 0/90 and $45/-45$ deg were fabricated with 10% volume fraction of graphite powder added to the epoxy.

2) High thermal conductivity (HTC) samples were made with a Mitsubishi FT3C116 woven mat made of coal pitch-based K13C1U carbon fibers and cured with Bryte EX-1510 cyanate ester epoxy. Samples were made with angles of 0/90, $45/-45$, and from $25/-25$ to $65/-65$ in 5 deg increment. Samples of 0/90 and $45/-45$ were also fabricated with 10% volume fraction of graphite powder added to the epoxy.

3) Unitape samples (UNI) were fabricated with Mitsubishi K13C1U carbon fibers and cured with Bryte EX-1510 cyanate ester epoxy.

HTC and UNI samples were made with the same materials used by Entech in the current model of the SLASR to obtain a more accurate representation of the effect of the weave angle variation in the thermal conductivity of the samples.

The standard lay-up procedure for the fabric sample preparation was followed. The procedure consists of "sandwiching" the epoxy-impregnated carbon fiber cloth between two layers of De-comp D200 release fabric (peel ply), three layers of De-comp D3000-4 breather/bleeder cloth (breather cloth) and two sections of De-comp D230 bagging film (vacuum bag) sealed on the edges with De-comp D312 sealant tape and secured on an aluminum mold plate. A vacuum foot was installed on the plate over a small separate section of breather cloth.

The basics of sample preparation consist of applying one layer of Teflon coated peel ply and a layer of breather cloth on each side of the impregnated fabric. The peel ply is permeable to the epoxy resin, and the breather cloth allows the absorption of any excess resin. Under vacuum, the force applied over the fabric moves any excess resin away from the fiber, thus obtaining a very thin sheet of cured carbon fiber composites. Sample thickness was measured in 10 points and then averaged for each sample to check for uniformity. All samples had thickness between 0.2794 and 0.3810 mm (11 and 15 mils). Thinner samples would be obtained with the use of an autoclave and vacuum molding.

The Unitape sample was prepared on a filament winder. The pitch and speed of the winder were set on the electronic controller to pull the fiber from the K13C1U tow (1 k tow count) without breaking the fibers. A constant tension spool was used to keep the fibers straight under a load of approximately 18 N (4 lbs). Peel ply was applied over the Unitape, and then it was transferred to a mold plate and vacuum bagged following the same procedure as in the fabric samples.

The samples created and their dimensional characteristics are listed in Table 1. A sample of eGraf spreadershield with a 0.0127 mm (0.5 mil) Mylar coating on one side was also obtained and tested in the same manner as the carbon fiber composites. Figure 4 shows a schematic of the alignment of the fibers in the samples and nomenclature used for the name of each one.

B. Test Facility

The test facility for in-plane conductivity measurement consists of two steel plates with a sample clamp and five type-K thermocouples in each plate to estimate heat flow in and out of the samples. The thermocouples were attached to the fluxmeter with E3081 single-component epoxy in 1.587 mm (1/16 in.) diameter indentations made on the midline of the plates. Heat was supplied through an electrical heater attached to one of the plates. Experiments were run in vacuum to minimize convective losses along with a radiation shield to minimize interchange with the environment.

The experimental apparatus consisted of a frame with sliding plates that supported the heat source and sink, the specimen holder assemblies, and the test samples as shown in Fig. 5. Uniform contact pressure over the test sample interfaces was assured by the use of two clamps with four screws each to hold the sample into the fluxmeter assemblies. Thermal grease was used to minimize contact resistance at the interfaces. An electric kapton heater with nominal power of 120 W was placed in the lower fluxmeter holder to provide the heat flux, while coolant (ethylene glycol) was circulated through the upper fluxmeter holder. To avoid convection losses, the entire test facility was housed in a vacuum of 5×10^{-3} torr maintained by an oil diffusion pump. Further, radiative losses from the fluxmeters and samples were reduced by placing a thermal insulator and radiation shield around the vertical test column.

C. Experimental Procedure

The effective thermal conductivity was determined by using upper and lower heat fluxmeters made of ASTM 1095 spring steel plate of 3.175 m (1/8 in.) thickness. The fluxmeters were instrumented with 30-gauge, Tefon® sheath, special limit of error type K-chromel/alumel thermocouples to enable the calculation of the temperature gradient, the temperature difference across the composite, and the heat flux into the samples. Thermocouples were spaced evenly at 10 mm (0.3937 in.) over the fluxmeters with additional thermocouples located on the edge of the sample clamps and below the heater.

Heat input to the samples was controlled with a Variac power supply. Two measures of thermal conductivity were performed on each sample with power inputs of 4.5 and 10.3 W (12 and 24 V, respectively), which correspond to the power range expected from each cell of the SLASR array. Each test was run for 12 h, first at 4.5 W input power and then at 10.3 W input power. Steady state—less than

Table 1 Sample description

Sample	Avg. thickness	Sample size	Avg. volume frac.[a]
Low thermal conductivity (LTC) samples:			
0/90	0.297 mm (11.7 mils)	196 × 76.2 mm (8 × 3 in.)	55.7%
45/ − 45	0.297 (11.7)	196 × 76.2	55.7%
0/90 w/graphite filler	0.355 (14.0)	196 × 76.2	46.6%
45/ − 45 w/graphite filler	0.355 (14.0)	196 × 76.2	46.6%
30/ − 30	0.305 (12.0)	196 × 76.2	54.4%
60/ − 60	0.305 (12.0)	196 × 76.2	54.4%
High thermal conductivity (HTC) samples:			
0/90	0.279 mm (11.0 mils)	196 × 101.6 mm (8 × 4 in.)	36.4%
45/ − 45	0.279 (11.0)	196 × 101.6	36.4%
0/90 w/graphite filler	0.338 (13.3)	196 × 101.6	30.1%
45/ − 45 w/graphite filler	0.340 (13.4)	196 × 101.6	29.8%
40/ − 40	0.292 (11.5)	196 × 101.6	34.8%
50/ − 50	0.292 (11.5)	196 × 101.6	34.8%
35/ − 35	0.287 (11.3)	196 × 101.6	35.4%
55/ − 55	0.205 (12.0)	196 × 101.6	33.4%
30/ − 30	0.302 (11.9)	196 × 101.6	33.6%
60/ − 60	0.307 (12.1)	196 × 101.6	33.0%
25/ − 25	0.333 (13.1)	196 × 101.6	30.6%
65/ − 65	0.333 (13.1)	196 × 101.6	30.6%
Unitape (UNI) samples:			
Unitape	0.200 mm (7.9 mils)	196 × 101.6 mm (8 × 4 in.)	31.6%
eGraf spreadershield (SS)	0.140 (5.5)	196 × 76.2	90.1%

[a]Volume fraction based on 25% void volume in the fabric (previously measured in FT3C116 fabric) and considering as matrix any additional thickness.

0.2 deg change in 1 h—was reached in approximately 3 h. All samples were run a minimum of 6 h.

A 0.3048 mm (12 mils) thickness ASTM B209 aluminum foil was also measured to test the accuracy of the experimental setup. All the data were collected with a data acquisition system and recorded on a computer using a Labview interface.

D. Uncertainty Analysis

The Holman [17] method, based on the Kline and McClintock [18] work, was employed to determine the overall relative uncertainty in the effective thermal conductivity of the composites according to Eq. (1).

$$W_p = \sum_{i=1}^{n} \left[\frac{\partial P}{\partial x_i} (W_i) \right]^2 \tag{1}$$

where P is the nominal conductivity equation, W_x is the uncertainty of variable x, and i represents all the variables in the nominal relationship.

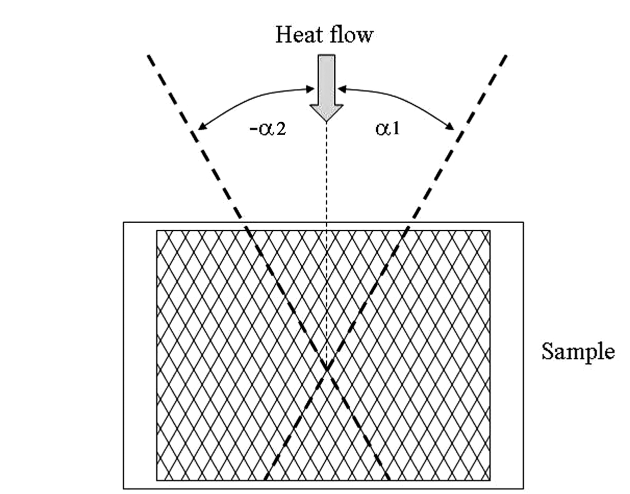

Fig. 4 Schematic of the fiber alignment of the samples.

The overall uncertainty in the reported values of thermal conductivity of the CFC comprises various parameters, including the uncertainty in the heat flux (0.1 W); the location tolerances for the thermocouples; effective length and thickness of the samples (0.5 mm, 0.2 mils); and the temperature readings (1 K). The average overall uncertainty of the effective thermal conductivity of each sample was approximately 9.4%.

V. Results and Analysis

Figures 6 and 7 show the experimental results for LTC and HTC/Unitape samples. Thermal conductivity and average temperature of the samples are shown in Table 2.

Figures 8 and 9 take the same data used in Figs. 6 and 7, but assume that enough time and resources are available, such as the autoclave and vacuum use, to reduce the thickness of the samples to 0.127 mm (5 mils). Whereas 99% of the heat conduction occurs in the fibers, the same amount of heat can be carried in a thinner material, leading to a higher effective thermal conductivity. The thermal conductivity of the epoxy matrix was, therefore, neglected in this study.

The Unitape sample conductivity was projected to a thickness of 0.0635 mm (2.5 mils), instead of 0.127 (5 mils), due to the fact that Unitape is commercially available in said thickness. This is the reason why in Fig. 7 the eGraf sample has the higher (measured) conductivity, while in Fig. 9 the higher value (projected) corresponds to the Unitape.

The ASTM B209 aluminum foil was tested with power inputs of 1.1, 4.5, and 10.3 W, yielding thermal conductivities of 196.8, 205.0, and 210.7 $W/m \cdot K$, respectively. The standard value of thermal conductivity for this type of aluminum is 193.0 $W/m \cdot K$, which shows good accuracy of the experimental method employed in this work.

Figure 10 shows the measurements on the 0–90 samples compared to the models of Rayleigh, Singh, and Alexander, as given by Eqs. (2–4), respectively,

$$\frac{K}{K_f} = 1 - \frac{2(1-\nu)}{\Gamma + (1-\nu) - \frac{0.0361(1-\nu)^4}{\gamma} \frac{0.0134(1-\nu)^8}{\gamma}} \tag{2}$$

where $\gamma = (\beta + 1)/(\beta - 1)$, and $\beta = (k_f/k_m)$. The sub indices f and m indicate the property of the fiber and matrix, respectively.

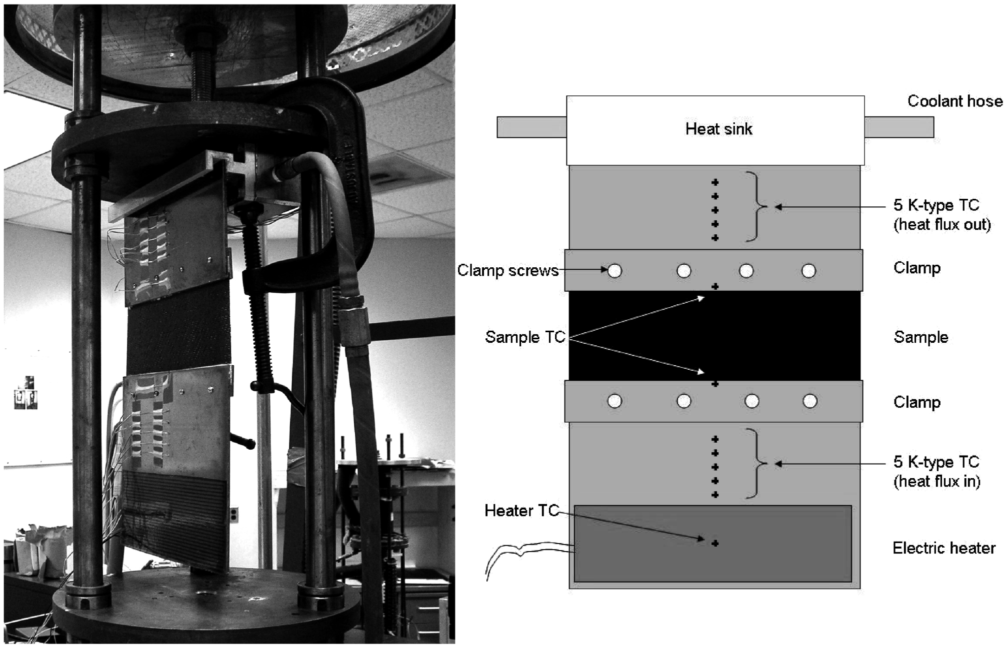

Fig. 5 Experimental setup and schematic for thermal conductivity test.

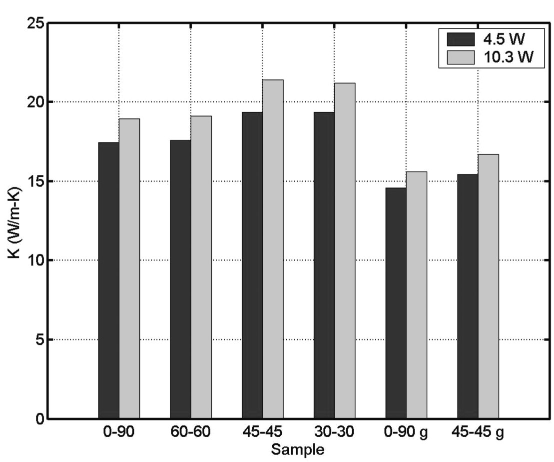

Fig. 6 Measured thermal conductivity of LTC samples.

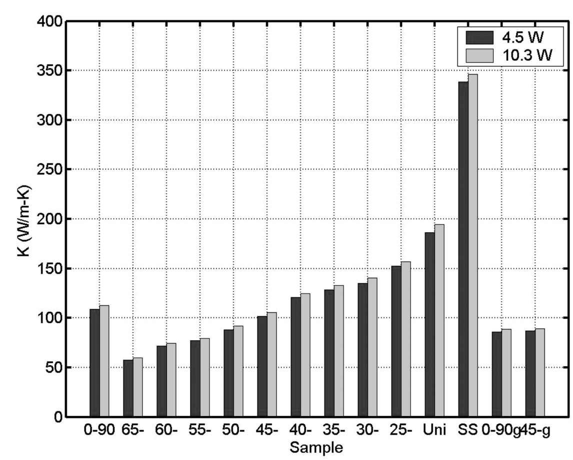

Fig. 7 Measured thermal conductivity of HTC samples.

$$\frac{k}{k_m} = \left[\beta\nu + (1-\nu)\exp\left(1-\sqrt{\frac{1}{\beta}}\right)^{b}\right]\exp\left[(\nu-1)\left(1-\sqrt{\frac{1}{\beta}}\right)^{b}\right] \tag{3}$$

where the exponent $b = 20\sqrt{\frac{1}{\beta}}$; and finally

$$\frac{k}{k_m} = (\beta)^{(\nu)^{\psi}} \tag{4}$$

where the exponent ψ is 0.34 for fiber materials.

In general, there is reasonable agreement between the correlations and the HTC samples, where the Rayleigh correlation predicted conductivity 25% higher than the measured values. Singh's correlation gave slightly higher values, while Alexander's relationship predicted values on the order of 50% of the experimental data. Table 3 shows the experimental values on the 0–90 HTC sample, as well as all the correlations used for the analysis.

The rule of mixtures predicted values 2 times bigger than the experiments; Maxwell's correlation gave values close to that of the epoxy matrix, while Soliman's relationship showed values close to the fibers alone for the HTC samples. The prediction for the LTC samples were off by a factor of 6, which was expected considering the measured conductivity on the LTC was much higher than the fibers alone. One possible explanation is that the effective conductivity of the fibers in the LTC sample is higher than the reported manufacturer's value (6.8 $\mathrm{W/m \cdot K}$).

Results on the 0.3048 mm (12 mils) thick AS4 samples (low thermal conductivity fibers) indicate that in-plane thermal conductivity can be improved up to 15% by varying the fiber orientation. Changing fiber orientation from $0/90$ to $45/-45$ (i.e., rotating the sample with respect to the heat flow direction) allows more fibers to become involved in the heat spreading, improving overall conductivity. As expected, when the fiber angle, with respect to heat flow direction, is lower $(30/-30)$ the thermal conductivity increases slightly. The opposite effect was observed when the angle was increased $(60/-60)$.

The weave angle effect on the graphite filled samples was the same, though the powder increased the overall thickness of the samples from 0.3048 to 0.3556 mm (12 to 14 mils), thus increasing the cross sectional area and reducing the overall effective thermal conductivity. However, the graphite filled samples were less porous and might have better emissive properties.

Although changing the weave angle of the low thermal conductivity fibers had very little effect on the composite thermal conductivity, probably because of the large fraction of the heat conduction occurred through the matrix, changing the weave angle

Table 2 Experimental results

Sample	4.5 W k (temp.)	10.3 W k (temp.)
Low thermal conductivity (LTC) samples:		
0/90	17.44 W/m · K (32.2°C)	18.95 W/m · K (52.6°C)
45/ − 45	19.37 (30.9)	21.36 (50.9)
0/90 w/graphite filler	14.57 (32.0)	15.61 (52.8)
45/ − 45 w/graphite filler	15.45 (31.4)	16.69 (51.2)
30/ − 30	19.35 (31.0)	21.19 (51.8)
60/ − 60	17.58 (31.9)	19.12 (51.4)
High thermal conductivity (HTC) samples:		
0/90	108.86 W/m · K (16.7°C)	112.64 W/m · K (25.2°C)
45/ − 45	101.82 (16.5)	105.75 (24.5)
0/90 w/graphite filler	86.13 (16.2)	88.58 (24.5)
45/ − 45 w/graphite filler	86.97 (16.5)	89.13 (24.4)
40/ − 40	121.12 (16.8)	124.84 (24.7)
50/ − 50	88.13 (17.0)	92.14 (25.2)
35/ − 35	128.73 (15.6)	132.92 (23.6)
55/ − 55	77.41 (16.9)	79.42 (25.7)
30/ − 30	134.99 (15.7)	140.47 (21.3)
60/ − 60	71.75 (16.81)	74.26 (25.9)
25/ − 25	152.71 (14.0)	157.05 (20.8)
65/ − 65	57.45 (14.3)	59.72 (24.5)
Unitape (UNI) samples:		
Unitape	186.54 W/m · K (16.2°C)	194.29 W/m · K (23.6°C)
eGraf spreadersheild (SS)	338.5 (14.3)	——

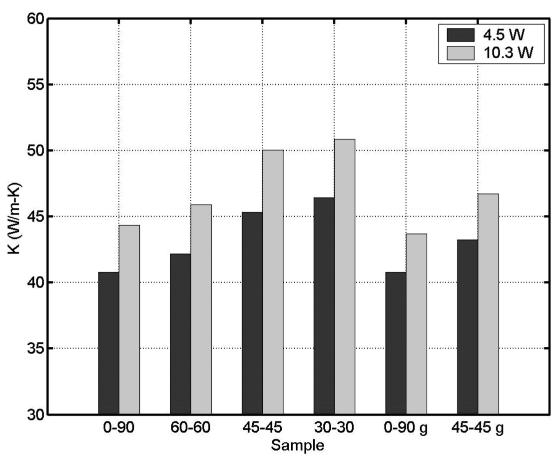

Fig. 8 Projected thermal conductivity of LTC samples.

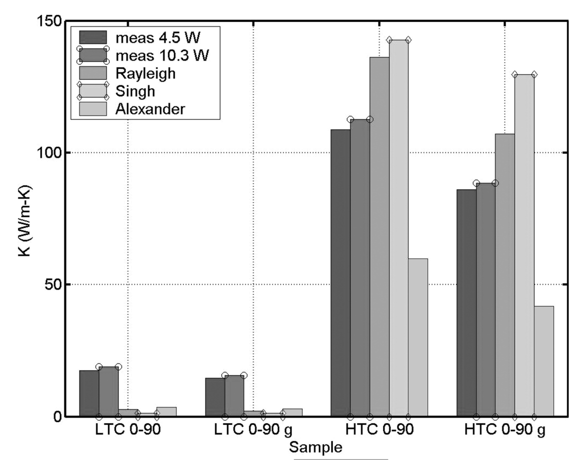

Fig. 10 Experiment data vs analytical/empirical models.

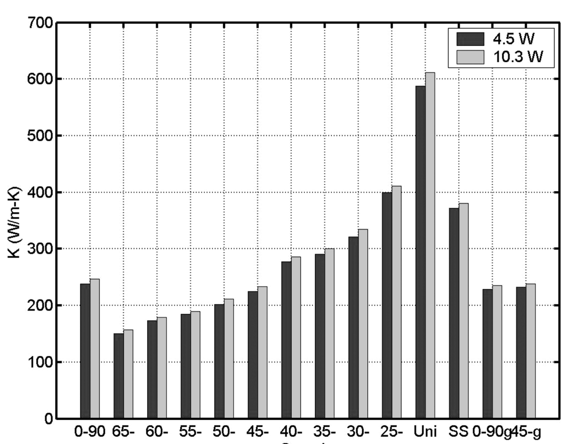

Fig. 9 Projected—to 5 mils thickness—thermal conductivity of HTC samples. (*) Unitape projection to 2.5 mils.

for the high conductivity fibers had a large effect on the composite thermal conductivity.

The 45/ − 45 sample was identical to the 0/90 baseline, except it was rotated 45 deg with respect to the direction of heat flow. Its performance was slightly worse (0.93) than the baseline because the effective length of the heat path was higher. The thermal energy flows almost exclusively through the fibers, none of which are aligned with the direction of heat flow. So, the effective path length is $1/\cos(45\ \mathrm{deg})$ times the straight path length, giving a thermal

Table 3 Experimental data vs empirical correlations

Description	k, W/m · K
HTC 0-90 measured, 4.5 W (16.7°C)	108.86
HTC 0-90 measured, 10.3 W (25.2°C)	112.64
Rayleigh	136.28
Singh	142.71
Alexander	59.86
Rule of mixtures [11]	225.81
Maxwell [13]	0.54
Soliman [14]	608.89

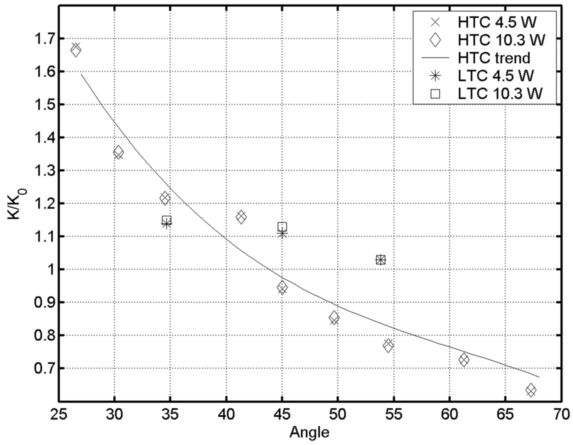

Fig. 11 Relative thermal conductivity. Values relative to the 0/90 sample.

conductivity per ply of 0.7 times that of the baseline. In the 45-45 sample fibers from both plies of the panel are involved in the heat transfer, so the thermal conductivity should be improved ~1.4 times (2 × 0.7); however an angled path also implies more truncated fibers extending under only one steel plate (heater or cooler), thus reducing the effective thermal conductivity.

As expected and predicted, the effective thermal conductivity of the composite decreased as the fiber angle increased above 45 deg and increased as the angle decreased below 45 deg. In the limiting case of the Unitape, all of the fibers were aligned with the heat flow, and the composite achieves a projected thermal conductivity of 400 W/m · K. In fact, there seems to be a linear correlation between weave angle and composite thermal conductivity. The increased effect of the weave angle in the high conductivity fiber samples was due to the much higher fraction of the heat load carried by the fibers in those samples.

We define the relative thermal conductivity (k/k_0) as the ratio between the thermal conductivity of each sample relative to that of the 0/90 sample. Figure 11 shows the values of k/k_0 as a function of the *measured* angle. Samples were fabricated with nominal angles from 25/ − 25 to 65/ − 65 in 5 deg increments, but once the samples were cured and cut, the final angle was measured in 10 different points of each sample by scanning and using computer software. It can be appreciated in Fig. 11 that most of the samples were within ±1 deg of the nominal value, with samples 25/ − 25, 40/ − 40, and 65/ − 65 showing higher deviations up to 2.4 deg.

It can be observed that, with exception of the 40/ − 40 sample, all the data points for the HTC follow the polynomial equation:

$$\frac{k}{k_0} = -0.000012\alpha^3 + 0.002194\alpha^2 - 0.144530\alpha + 4.130945$$

where α is the angle of the fibers relative to the heat flow direction. It can also be observed that for LTC samples the influence of the angle of the fibers was not as significant as in the HTC. Even though only three data points were obtained for the LTC samples, it was clear they do not follow the same equation as in the HTC sample; the reasons for this may be as follows:

1) LTC samples were made with AS-4, PAN-based low thermal conductivity fibers. The relative effect of the epoxy matrix, which is independent of the angle of the fibers and neglected in this study, may play a bigger role in the overall conductivity of the LTC samples.

2) LTC fibers are more thermally resistant along the fiber (i.e., less thermally conductive), so it is expected that the contact resistance between fibers be higher too; therefore, there is more resistance for the heat flow going from one layer or strand to the next in the thru-plane direction, hence reducing overall thermal conductivity for the samples.

3) AS-4 fibers are "hairy," having small fibrils that may increase transverse conductivity and reduce the effect of the fiber angle.

The disparity in the behavior of the relative thermal conductivity for the HTC and LTC seems to indicate that the correlation for thermal conductivity as a function of the angle of the fibers is specific for each combination of fibers epoxy, and that to develop a single equation to predict the thermal conductivity of a composite, other variables should be taken into account.

One area that requires more investigation is the structural properties of the Unitape. The thermal conductivity meets the requirements for this task, but we did not have resources to quantify the structural characteristics of this material, or examine methods for stiffening the material. We created a sample of Unitape with two AS4 fiber ribs for stiffening, but did not have time to test its stiffness.

VI. Conclusions

It was determined that changing the fiber angle was an effective way to increase the overall thermal conductivity of the carbon composite material tested, and furthermore this allows for a reduction in the overall thickness (i.e., mass) of the radiator panel. The fiber type and fiber angle significantly affected the in-plane thermal conductivity of thin carbon fiber composites. Samples with low thermal conductivity were experimentally tested with PAN-based fibers ($k = 6.8$ W/m · K) in a Fiberglast epoxy resin, and high thermal conductivity samples tested with coal-pitch-based fibers ($k = 620$ W/m · K) in a cyanate ester resin. Samples were fabricated from 0/90 woven cloths and warped to obtain a range of fiber-pattern angles from 25/ − 25 to 65/ − 65. The filler effect on thermal conductivity was evaluated on additional LTC and HTC samples prepared with 10% volume fraction of graphite powder in the epoxy matrix. The measured thermal conductivity of LTC samples ranged from 15–20 W/m · K which showed a maximum improvement of 15% as the angle of the fibers relative to the heat flux direction was varied from 0/90 to 30/ − 30. HTC samples showed thermal conductivities between 60 and 150 W/m · K, with an improvement up to 60% when the angle of the fibers was changed from 0/90 to 25/ − 25. The samples with graphite powder showed no significant enhancement in thermal performance as the filler material increased the thickness of the samples, thus increasing the cross sectional area and reducing the effective thermal conductivity. Measured thermal conductivity on the 0/90 HTC samples was compared to a few models. The *rule of mixtures* model (analytical) predicted values 2 times bigger than the experiments, whereas *Rayleigh* correlation (empirical) predicted conductivity 25% higher than the measured values. As potential alternatives for aerospace applications, unidirectional tape and eGraf's Spreadershield® foils were also tested, both specimens showed very good thermal performance. Moreover, the investigation revealed that Unitape will meet the mass and heat transport requirements set out for the SLASR program. Further research is needed to assess whether the characteristics of the Unitape satisfy the structural requirements of the SLASR.

Acknowledgements

We would like to acknowledge the contributions of Scott Coughlin, graduate student at Texas A&M College Station, and Vishwajit Gudge, graduate student at Texas A&M—Kingsville, for their help in the modeling and experimental work.

References

[1] O'Neill, M. J., McDanal, A. J., Piscozor, M. F., Edwards, D. L., Eskenazi, M. I., and Brandhorst, H. W. "Recent Technology Advances for the Stretched Lens Array (SLA): A Space Solar Array Offering State of the Art Performance at Low Cost and Ultra-Light Mass," *31st IEEE Photovoltaic Specialist Conference*, IEEE, Piscataway, NJ, Jan. 2005.

[2] O'Neill, M. J., "1000 W/kg Solar Concentrator Arrays for Far-Term Space Missions," *Space Technology & Applications International Forum (STAIF 2004)*, Institute for Space Nuclear Power Studies, University of New Mexico, Albuquerque, NM, Feb. 2004.

[3] Scott, E. P., and Beck, J. V., "Estimation of Thermal Properties in Epoxy Matrix/Carbon Fiber Composite Materials," *Journal of Composite Materials*, Vol. 26, No. 1, 1992, pp. 132–149.

[4] Mirmira, S. R., Jackson, M. C., and Fletcher, L. S., "Effective Thermal Conductivity and Thermal Contact Conductance of Graphite Fiber Composites," *Journal of Thermophysics and Heat Transfer*, Vol. 15, No. 1, 2001, pp. 18–26.

[5] Kulkarni, M. R., and Brady, R. P., "A Model of Global Thermal Conductivity in Laminated Caron/Carbon Composites," *Composite Science and Technology*, Vol. 57, Aug. 1997, pp. 277–285.

[6] Ohlhorst, C., Vaughn, W., Ransone, P., and Tsou, H., "Thermal Conductivity Database of Various Structural Carbon-Carbon Composite Materials," NASA TM 4787, Nov. 1997.

[7] Gaier, J., Stueben, H., Berkebile, S., and Balagadde, F., "Electrical and Thermal Conductivity of Carbon Fiber-Polymer Composite Plates," *9th International Conference of Composites Engineering*, 2002, pp. 217–218.

[8] James, B. W., Wostenholm, G. H., Keen, G. S., and McIvor, S. D., "Prediction and Measurement of the Thermal Conductivity of Composite Materials," *Journal of Physics D: Applied Physics*, Vol. 20, No. 3, 1987, pp. 261–268.

[9] Ibrahim, A., "Fabrication, Testing and Evaluation of High-Thermal-Conductivity, Lightweight Polymer Composite Reinforced with Pitch Graphite Fibers as Heat Sink for High Density Packaging Applications," *6th International Society for the Advancement of Material and Process Engineering Electronics Conference*, SAMPE, San Diego, CA, 1992, pp. 556–567.

[10] Jensen, G. A., "Application of High Conductive Graphite/Epoxy for a Spacecraft Thermal/Structural Radiator," *Proceeding of the 23rd International Society for the Advancement of Material and Process Engineering Technical Conference*, Vol. 3, Society for the Advancement of Material and Process Engineering, Covina, CA, 1991, pp. 589–600.

[11] Peterson, G. P., and Fletcher, L. S., "A Review of Thermal Conductivity in Composite Materials," AIAA Paper AIAA-87-1586, 1987.

[12] Rayleigh, L., "On the Influence of Obstacles Arranged in Rectangular Order Upon the Properties of a Medium," *Philosophical Magazine*, Vol. 34, 1892, p. 481.

[13] Maxwell, J. C., *A Treatise on Electricity and Magnetism*, 3rd ed., Vol. 1, Oxford Univ. Press, reprinted by Dover, New York, 1954.

[14] Soliman, M. N., Graumann, D. W., and Berenson, P. J., "Effective Thermal Conductivity of Dry and Liquid-Saturated Sintered Fiber Metal Wicks," ASME Paper 70-HT-SpT-40, 1970.

[15] Singh, B. H., Dybbs, A., and Lyman, F. A., "Experimental Study of the Effective Thermal Conductivity of Liquid Saturated Sintered Fiber Metal Wicks," *International Journal of Heat and Mass Transfer*, Vol. 16, 1973, pp. 145–155.

[16] Alexander E. G., "Structure-Property Relationships in Heat Pipe Wicking Materials," Ph.D. Thesis, North Carolina State University, Department of Chemical Engineering, Raleigh, NC, 1973.

[17] Holman, J. P., "Experimental Methods for Engineers," 5th ed., McGraw–Hill, New York, 1989.

[18] Kline, S. J., and McClintock, F. A., "Describing Uncertainties in Single-Sample Experiments," *Mechanical Engineering*, Vol. 75, 1953, pp. 3–7.